

Heterogenizing palladium tetraiodide catalyst for carbonylation reactions

Ida Zicarelli,^{a,*} Raffaella Mancuso,^{a,*} Francesco Giacalone,^{b,*} Carla Calabrese,^b Valeria La Parola,^c
Alex De Salvo,^a Nicola Della Ca',^d Michelangelo Gruttadauria,^b and Bartolo Gabriele^{a,*}

^a *Laboratory of Industrial and Synthetic Organic Chemistry (LISOC), Department of Chemistry and Chemical Technologies, University of Calabria, Via Pietro Bucci 12/C, 87036 Arcavacata di Rende (CS), Italy*

^b *Department of Biological, Chemical and Pharmaceutical Sciences and Technologies (STEBICEF)- University of Palermo and INSTM UdR – Palermo, Viale delle Scienze, Ed.17, Palermo I-90128, Italy*

^c *Institute for the Study of Nanostructured Materials, CNR-Palermo, Via Ugo La Malfa 153, Palermo I-90128, Italy*

^d *Department of Chemistry, Life Sciences and Environmental Sustainability (SCVSA), University of Parma, Parco Area delle Scienze, 17/A, 43124 Parma, Italy*

Abstract

We report here the preparation of new heterogeneous PdI_4^{2-} -based catalytic systems (**PdI₄@MWCNT-imi-X**, **X = Br, I**), which have been shown to act as efficient and recyclable heterogeneous catalysts in a paradigmatic oxidative carbonylation reaction.³ The newly developed materials present the PdI_4^{2-} anion supported on an imidazolium network (imi) grown on multi-walled carbon nanotubes (MWCNTs), and have been fully characterized by several advanced techniques (including XPS and TEM). The activity of **PdI₄@MWCNT-imi-X** has been tested, in particular, in the oxidative monoaminocarbonylation of terminal alkynes with secondary amines to give high value added 2-ynamides.

Products have been obtained in fair to high isolated yields (50-84%) starting from differently substituted substrates. The catalyst could be easily recycled and showed a good efficiency even after the fourth recycle, when deactivation began to take place owing to the formation of inactive Pd(0) species, as confirmed by XPS analysis. In any case, very limited metal leaching occurred during the catalytic process, as assessed by hot and cold filtration test experiments and by ICP-MS analysis of the carbonylation products.

Introduction

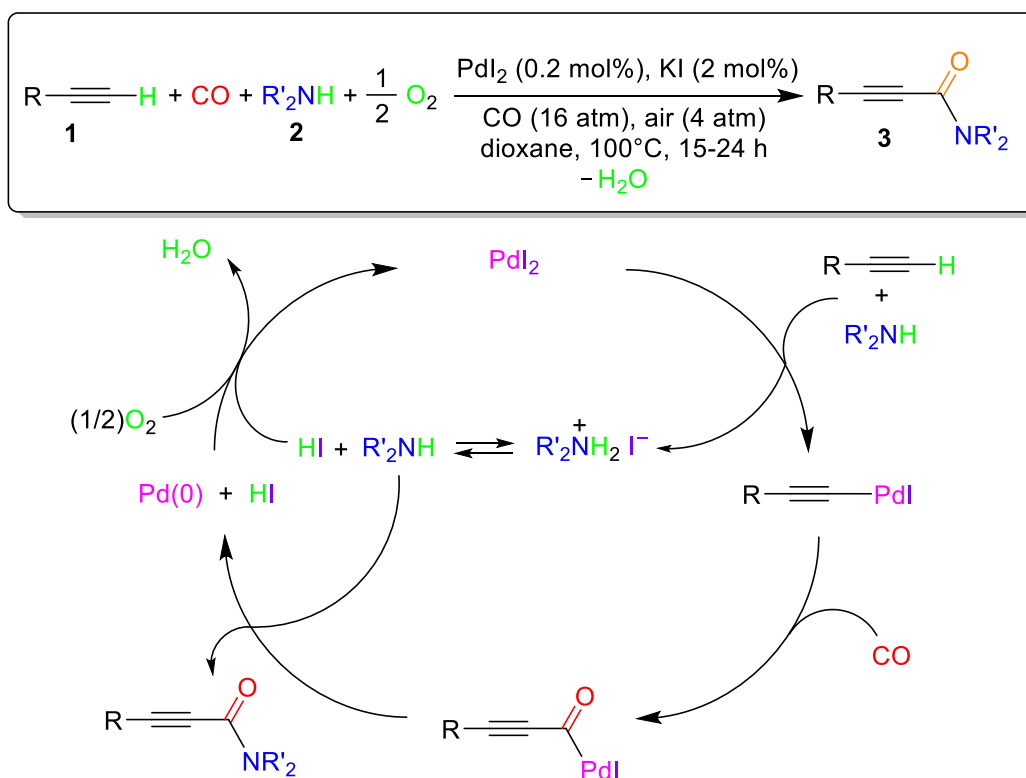
Carbonylation reactions with carbon monoxide or its surrogates are nowadays widely recognized as the most convenient and sustainable approach for the introduction of the carbonyl function into an organic substrate.^{1,2}

In the field of carbonylations, and oxidative carbonylations in particular, we have been active for many years. In 1992, we reported for the first time the use of a particularly simple homogeneous catalytic system, consisting of palladium iodide in conjunction with potassium iodide (PdI₂/KI, leading in situ to the catalytically active species PdI₄²⁻), for the oxidative dialkoxycarbonylation of propargyl alcohol.³ Since then, we have successfully used this catalytic system for the oxidative carbonylation of other terminal alkynes,⁴⁻⁶ as well as for the oxidative or non-oxidative carbonylation of functionalized alkynes leading to the direct synthesis of a plethora of carbonylated heterocyclic derivatives.^{7,8}

So far, however, no example of a PdI₄²⁻-based heterogeneous system has been developed and used in carbonylation reactions. On the other hand, a heterogeneous system like this would be particularly attractive if shown to be active in carbonylation processes under “true” heterogeneous conditions, which means, without any leaching of the catalytically active species in solution neither during the carbonylation process nor at the end of it, and therefore with no metal contamination in the liquid reaction phase. In fact, no or at least, negligible metal contamination would occur in this case in the final organic product, which is becoming a particular stringent requisite due to environmental constraints and for possible pharmacological applications.⁹

In the last years, carbon nanotubes (CNT) have emerged as useful scaffolds in the preparation of advanced nanostructured catalysts.¹⁰ CNT chemical functionalization through covalent modification represents an important tool for introducing well-distributed anchoring points and, is the first step toward the assembling of hybrid nanostructured materials with a hierarchical order. In this regard, hybrid CNT-poly ionic liquid networks have been successfully exploited as robust and recyclable catalysts.¹¹ In this work, we have successfully realized the heterogenization of “our” PdI₄²⁻-based catalytic system on CNT-poly ionic liquid networks to give new heterogeneous materials (**PdI₄@MWCNT-imi-X**, **X = Br, I**), which have been shown to act as efficient and recyclable heterogeneous catalysts in a paradigmatic oxidative carbonylation reaction.

In particular, we have tested their activity in the oxidative aminocarbonylation of terminal alkynes **1** with amines **2** to give 2-ynamides **3**,^{5,12} a process disclosed for the first time under catalytic conditions by our research group in 2001 using the homogeneous conditions with the PdI₂/KI catalytic system.⁵ 2-Ynamides represents key building blocks for the synthesis of a number of heterocyclic compounds¹³ and biologically active molecules.¹⁴ The carbonylation takes place through the formation of an alkynylpalladium species as the key intermediate from the reaction between the terminal alkyne, PdI₂ and the amine, as shown in Scheme 1 (anionic iodide ligands are omitted for clarity). This is followed by CO insertion, nucleophilic displacement by the amine, and palladium reoxidation. The latter occurs by oxidation, with molecular oxygen, used as external oxidant of 2 mol of HI formed during the process, to I₂, followed by oxidative carbonylation of the latter to Pd(0) to give back PdI₂ (Scheme 1). It is worth mentioning that, since our disclosure in 2001,⁵ the catalytic oxidative monoaminocarbonylation of terminal alkynes to 2-ynamides has been further elaborated by other research groups under different conditions and with larger alkyne scope with respect to our original paper.¹² However, it is also important to mention that in several cases the process has been carried out under conditions falling within the explosion range for CO/O₂ mixtures,^{12a-c,15} or requiring a stoichiometric amounts of a metal reoxidant (such as Ag₂O),^{12d} or under electrochemical palladium reoxidation conditions in the presence of phosphine ligands.^{12e} On the other hand, we have been able to apply our original method to a variety of alkynes bearing a suitably placed nucleophilic group, which allowed us to synthesize high value added carbonylated heterocycles in one step.¹⁶

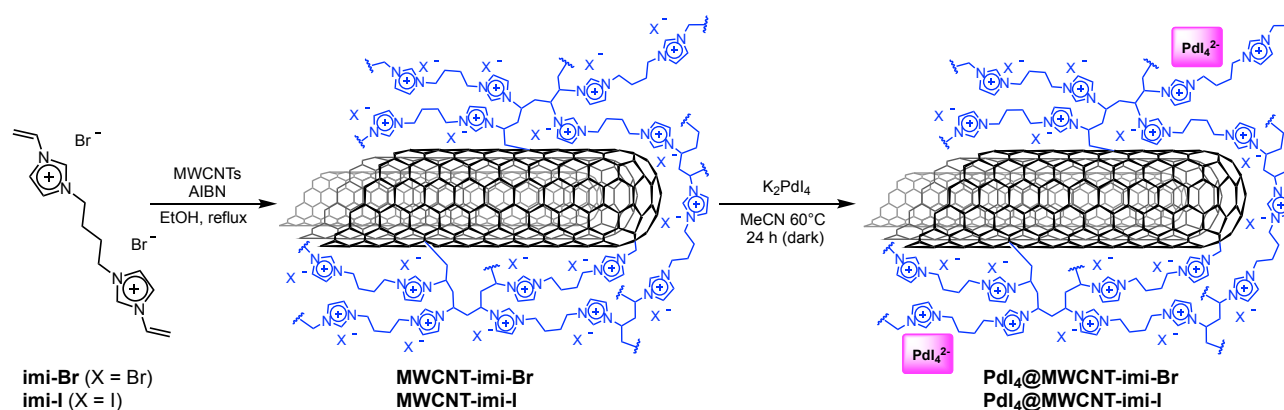


Scheme 1. PdI₂/KI-catalyzed oxidative monoaminocarbonylation of terminal alkynes to 2-ynamides **3** (anionic iodide ligands are omitted for clarity).⁵

Results and Discussion

Preparation and characterization of catalysts PdI₄@MWCNT-imi-X (X = Br, I)

In order to achieve an efficient heterogenization of PdI₄²⁻, we used **MWCNT-imi-X** (X = Br, I) as starting material, prepared by the reaction between 1,1'-(butane-1,4-diyl)bis(3-vinyl-1*H*-imidazol-3-ium) halide with multi-walled carbon nanotubes (MWCNTs) in the presence of AIBN in refluxing ethanol, as shown in Scheme 2.^{11a,17} Anion metathesis has been achieved by reacting **MWCNT-imi-X** with Na₂PdI₄ in acetonitrile to give **PdI₄@MWCNT-imi-X** (X = Br, I) (Scheme 2).



Scheme 2. Preparation of heterogeneous materials **PdI₄@MWCNT-imi-X** (X = Br, I).

The new materials obtained, **MWCNT-imi-Br** and **MWCNT-imi-I**, were characterized by means of several analytic and spectroscopic techniques. Thermogravimetric analysis (TGA) was employed both to evaluate the organic contents of the hybrid supports as well as the palladium content of **PdI₄@MWCNT-imi-X** (Figure 1). The polymer loadings were calculated by considering the net weight losses at 600 °C from TGA profiles under N₂ atmosphere (Figure 1, left). In particular, the polyimidazolium loading of **MWCNT-imi-Br** and for **MWCNT-imi-I** resulted to be 2.1 mmol/g and 1.7 mmol/g for, respectively. On the other hand, TGA analysis of **PdI₄@MWCNT-imi-Br** and **PdI₄@MWCNT-imi-I** under air flow (Figure 1, right) allow to estimate the Pd content since the small weight loss at around 800 °C can be accounted for by the quantitative decomposition of PdO to Pd.¹⁸ During the TGA experiment under air flow, all the organic material is burned down, while the palladium species are oxidized to PdO which is not stable over 800 °C.¹⁹ Hence a loading of 4.2 % w/w and 2.8 % w/w have been found for **PdI₄@MWCNT-imi-Br** and **PdI₄@MWCNT-imi-I**, respectively. Nevertheless, additional microwave plasma – atomic emission spectrometry (MP-AES) measurements on the two materials gave slightly minor values (3.32 % w/w and 2.61 % w/w), which will be used for the catalytic loading.

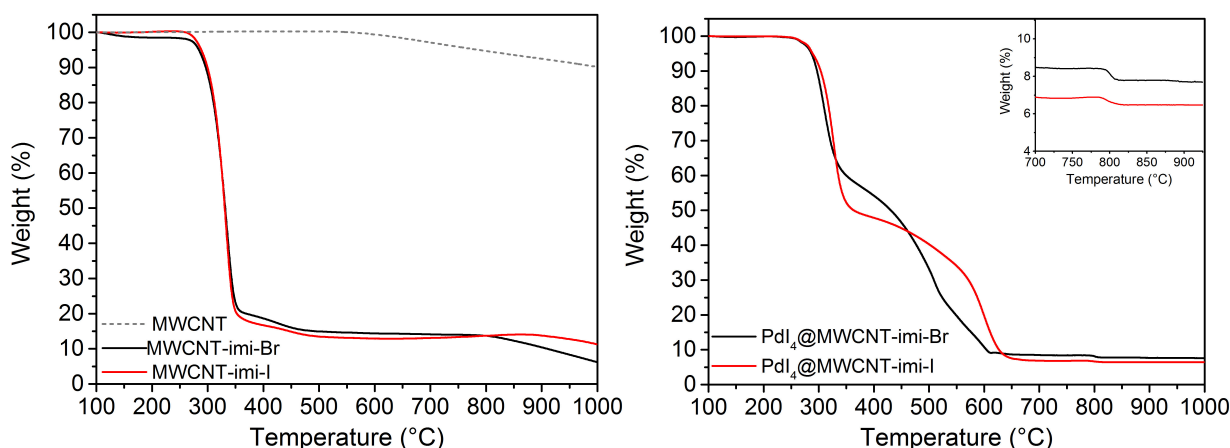


Figure 1. (left) Thermogravimetric analysis of MWCNT, **MWCNT-imi-Br** and **MWCNT-imi-I**, under nitrogen flow; (right) Thermogravimetric analysis of MWCNT, **PdI₄@MWCNT-imi-Br** and **PdI₄@MWCNT-imi-I** under air flow.

The XPS Pd 3d region (Figure 2) shows the spin orbit coupling Pd3d_{5/2} and Pd3d_{3/2} typical of Pd(II) with the two peaks at 337 eV (Pd3d_{5/2}) and 342.6 eV (Pd3d_{3/2}). The immobilization of PdI₄²⁻ on the support does not modify the chemical state of Pd.^{11a,20}

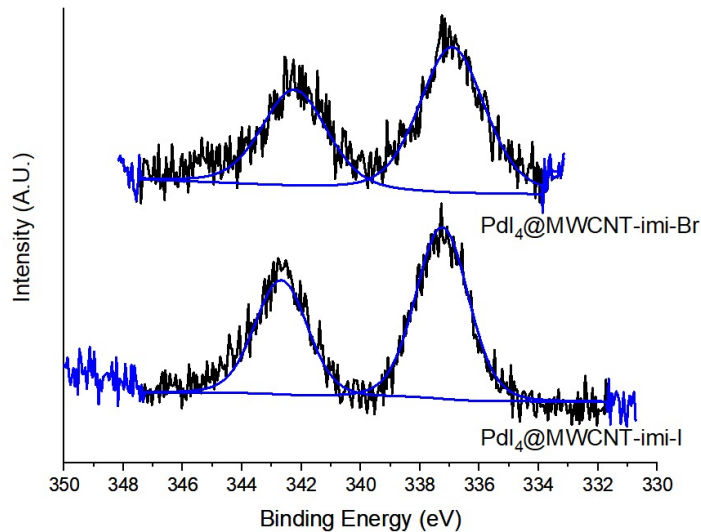


Figure 2. High-resolution XPS spectra of Pd 3d region of **Pdl₄@MWCNT-imi-Br** and **Pdl₄@MWCNT-imi-I**.

The morphological analysis of the two catalytic materials has been carried out by means of scanning transmission electron microscopy (STEM) (Figure 3). In order to obtain more information, the samples were analyzed with three different techniques simultaneously: the structural details of the samples were evaluated by transmitted electron (TE, images a and d), the morphological analysis was performed through secondary electron (SE, images b and e), while compositional homogeneity was evaluated by backscattered electrons (BS, images c and f). TEM images show that **Pdl₄@MWCNT-imi-Br** nano-objects are more aggregated with major size than **Pdl₄@MWCNT-imi-I**, which in turn looks very well dispersed (Figure 3a and 3d). SEM images (Figure 3b and 3e) give some insight into the three-dimensional shape of these aggregates whereas, more interestingly, in the backscattered electrons images the brighter parts are due to major number of electrons scattered by more electron-dense part of the materials, where PdI₄²⁻ ions are accommodated (Figure 3c and 3f). Thus, it seems clear that in both materials tetraiodopalladate ions are evenly distributed along the entire surface. A closer view to the support and the catalysts by means of TEM, show that all the materials display a similar morphology in which the carbon nanotubes are not visible since they are fully covered by the polymeric networks.

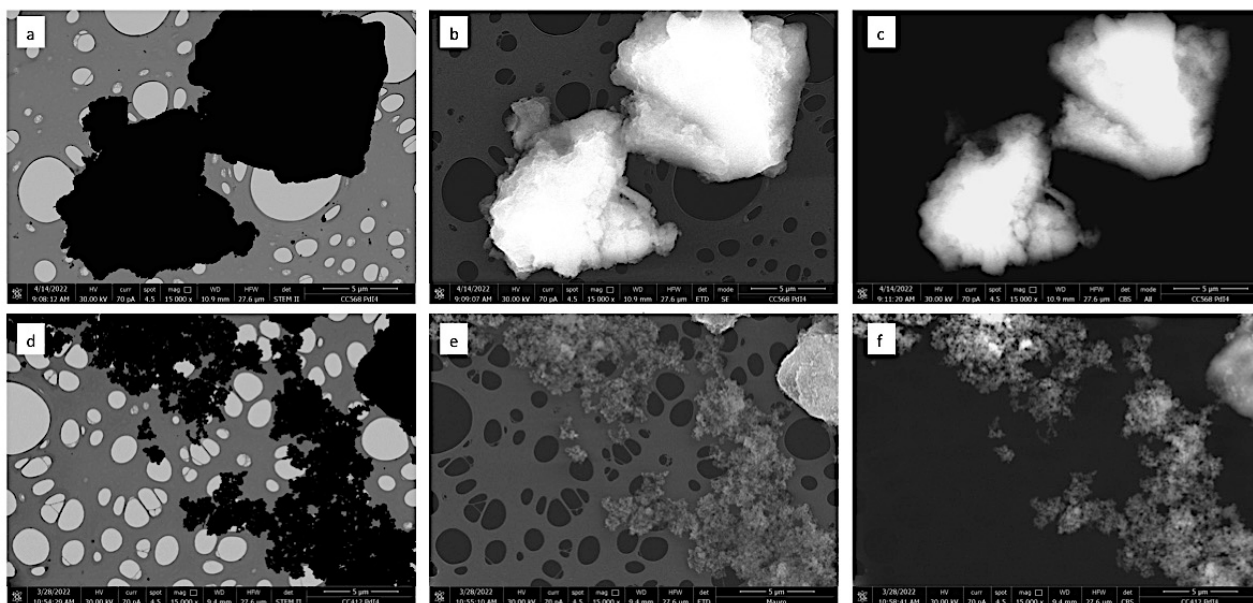


Figure 3. Morphological analysis of **PdI₄@MWCNT-imi-Br** (a, b, c) and **PdI₄@MWCNT-imi-I** (d, e, f): transmitted electron images (a and d); secondary electron images (b and e), backscattered electrons images (c and f).

Catalytic tests in the oxidative monoaminocarbonylation of terminal alkynes

We first assessed the catalytic activity of **PdI₄@MWCNT-imi-Br** in the oxidative monoaminocarbonylation of phenylacetylene **1a** with diethylamine **2a** to give *N,N*-diethyl-3-phenylpropiolamide **3aa**. With 2 mol% of **PdI₄@MWCNT-imi-Br** as heterogeneous catalyst and 1.2 equiv of **2a**, in dioxane as the solvent (0.5 mmol of **1a** per mL of dioxane), under 20 atm of a 4:1 mixture of CO-air,²¹ at 100 °C for 24 h, **3aa** was formed in 80% GLC yield (Table 1, entry 1). This initial result confirmed the catalytic activity of **PdI₄@MWCNT-imi-Br** for the monoaminocarbonylation reaction of terminal alkynes. The **3aa** yield was practically the same (81% by GLC) when the reaction was carried out under 40 atm total pressure (Table 1, entry 2), while it was lower when further increasing the total pressure to 60 atm (64% by GLC; Table 1, entry 3). A lower **3aa** yield was also observed with a catalyst loading of 1 mol% (65% by GLC; Table 1, entry 4). On the other hand, an 83% GLC yield of **3aa** was achieved under more diluted conditions (0.25 mmol of **1a** per mL of solvent; Table 1, entry 5). Under the last conditions, the process could also be conveniently carried out at 80 °C rather than 100 °C with a very good GLC yield of 81% (73% isolated, Table 1, entry 6).

In order to verify if the process really took place heterogeneously, we performed a hot filtration test experiment. Thus, a suspension of the catalyst in dioxane containing the substrate **1a** and diethylamine **2a** was heated at 80 °C for 1 h with stirring in a sealed tube. Then, the mixture was filtered still hot through a *Millipore* filter (0.2 μm in PTFE) and the autoclave was loaded with the filtered liquid phase. The mixture was allowed to react under the same conditions as those of Table 1, entry 6. At the end of the process, the GLC-MS of the crude showed the formation of very small amounts of **3aa** (<5%). This result clearly confirmed that the **PdI₄@MWCNT-imi-Br** – catalyzed carbonylation process did take place in a heterogeneous fashion.

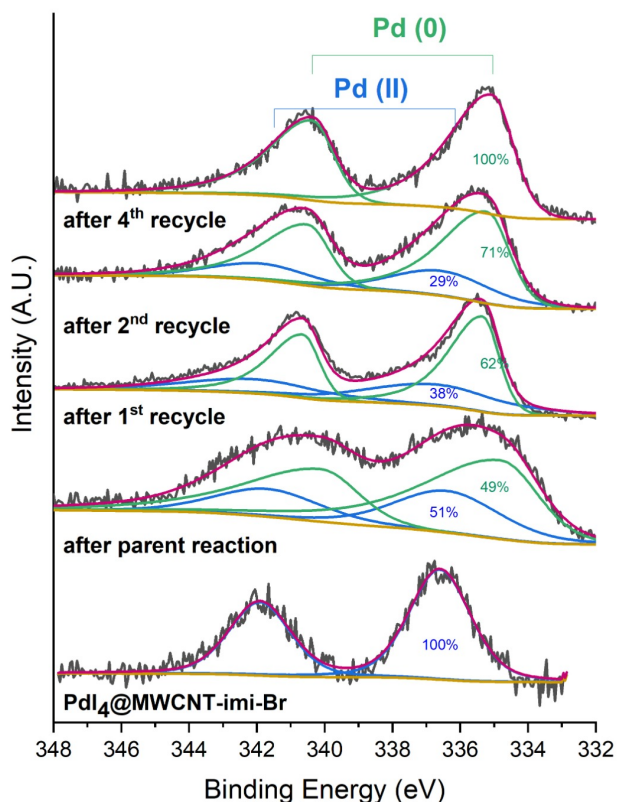
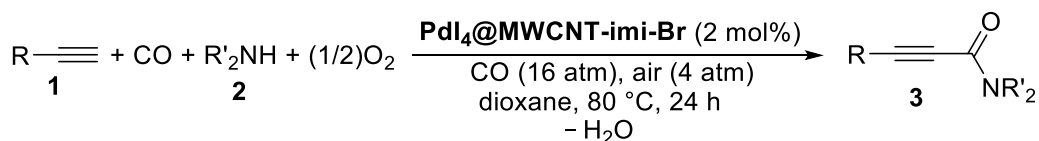
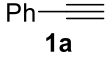
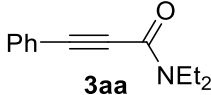
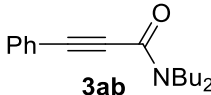
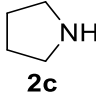
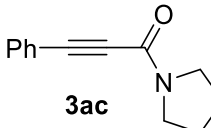
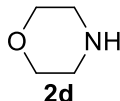
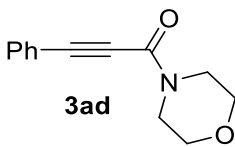
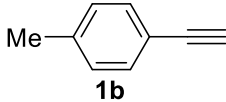
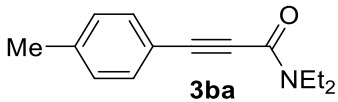
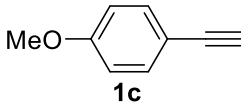
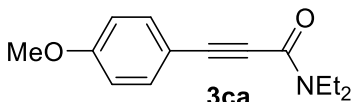
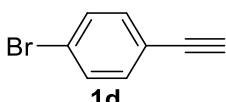
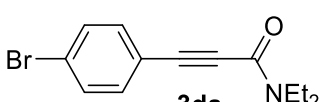


Figure 5. XPS spectra of pristine **PdI₄@MWCNT-imi-Br** and of the catalyst after the parent experiment and the first, second, and fourth recycle (carbonylation conditions are those reported in Table 1, entry 6).

The process was then extended to the use of other secondary amines **2b-d** and substituted phenylacetylenes **1b-d**; the results obtained are shown in Table 2. As can be seen from Table 2, entries 1-4, the process was quite general with respect to the nature of the amine, even though (as already observed in the original PdI₂/KI-catalyzed reaction)⁵ it did not work for non-nucleophilic, sterically hindered amines such as diisopropylamine **2e** (Table 2, entry 5). On the other hand, good results were obtained with diethylamine **2a** using phenylacetylenes bearing either an electron-donating (Table 2, entries 6 and 7) or an electron-withdrawing (Table 2, entry 8) group.

Table 2. PdI₄@MWCNT-imi-Br – catalyzed oxidative aminocarbonylation of phenylacetylenes **1** with amines **2** to give 2-ynamides **3**.^a



Entry	1	2	3	Yield (%) ^b of 3
1		Et ₂ NH 2a		73
2	1a	Bu ₂ NH 2b		50
3	1a			63
4	1a			57
5	1a	<i>i</i> Pr ₂ NH 2e	NR ^c	-
6		2a		66
7		2a		68
8		2a		63

^a All reactions were carried out in dioxane (0.25 mmol of **1** per mL of solvent) at 80 °C for 24 h, under 20 atm of a 4:1 mixture of CO-air, in the presence of 2 mol% of Pd and 1.2 equiv of R'₂NH **2**. ^b Isolated yield based on starting **1**. ^c NR = No reaction.

Considering the importance of the iodide anions in promoting oxidative carbonylations,²² we proceeded in testing the activity of PdI₄@MWCNT-imi-I (Scheme 2, X = I). The reaction between *p*-methoxyphenylacetylene **1c** and diethylamine **2a**, carried out with this catalyst under the same conditions as those reported in Table 2, led to the formation of **3ca** with an isolated yield of 79% (Figure 6), to be compared to 68% obtained using PdI₄@MWCNT-imi-Br (Table 2, entry 7). As shown in Figure 6, the catalyst activity tended to decrease after the second recycle, with a **3ca** yield of 42%. However, working with a higher total pressure (CO/air = 32 atm/8 atm), the decrease of activity was much more limited, as the yield of **3ca** was 81% in the first (parent) experiment, and still 70% after the third recycle and 59% after the fifth recycle (Figure 6). This is probably due to a more efficient Pd(0) reoxidation in the presence of a higher amount of oxygen in the reaction mixture, as confirmed by the XPS data (Figure 7). As can be seen from

Figure 7, reoxidation of the Pd(0) to Pd(II) was not complete after catalytic reuse, however, the use of higher CO/air pressure ensured a more efficient oxidation with a better recover of the catalytic activity. In fact, the percentage of Pd(II) was still 56% after the 5th recycle under CO/air = 32/8 atm (Figure 7, right), while it was 40% already after the second recycle under CO/air = 16/4 atm (Figure 7, left). Interestingly, the morphology of the reused catalysts is perfectly retained after multiple cycles, as showed by TEM pictures (Figure SX3).

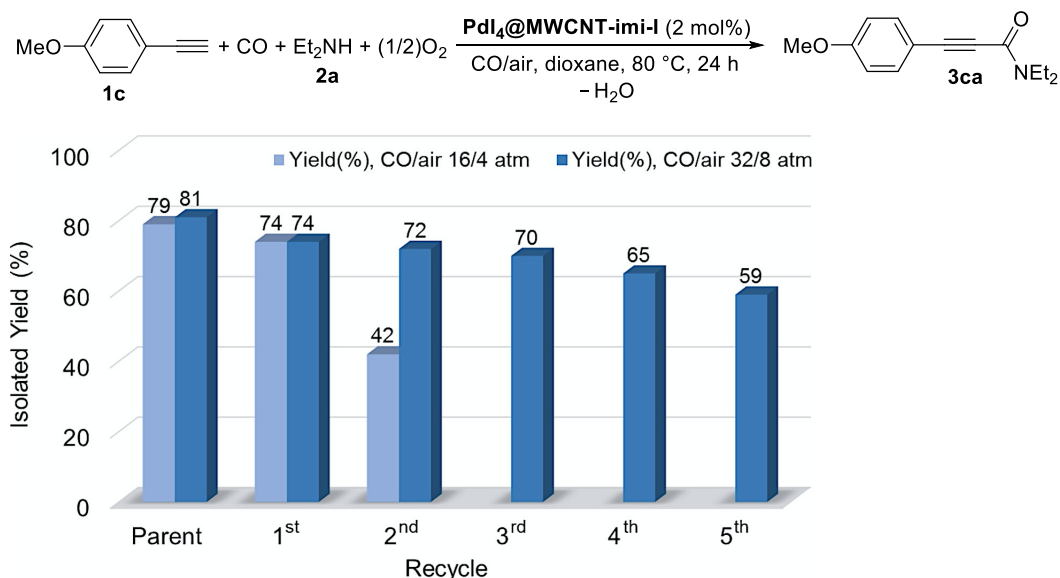


Figure 6. PdI₄@MWCNT-imi-I recycling experiments in the aminocarbonylation leading to **3ca** under CO/air = 16/4 atm (left) and 32/8 atm (right) (the other carbonylation conditions are those reported in Table 2).

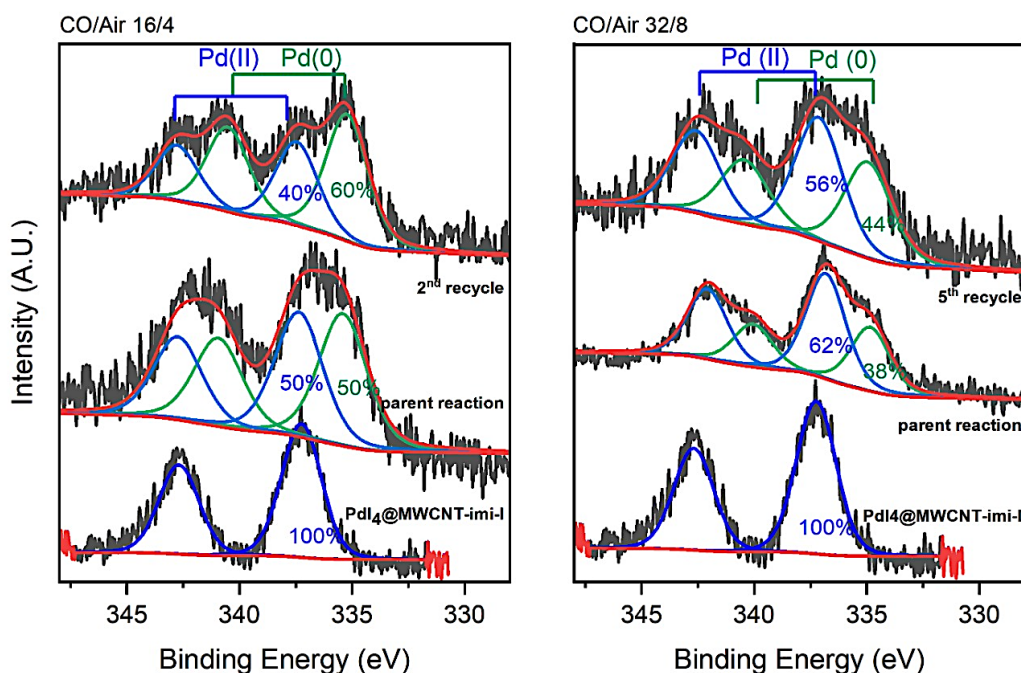
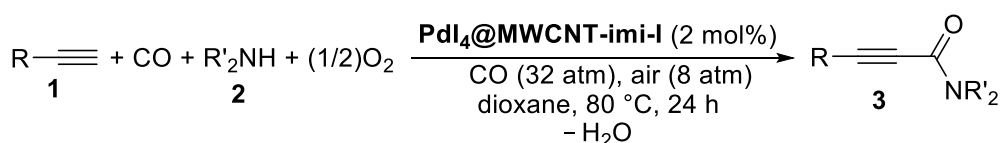
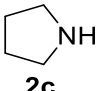
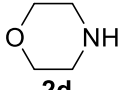
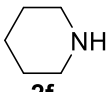


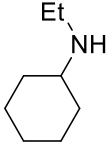
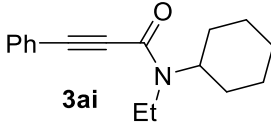
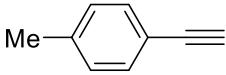
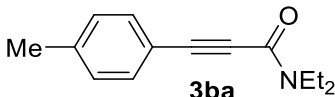
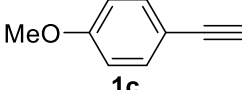
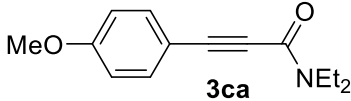
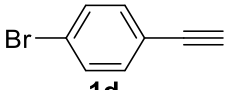
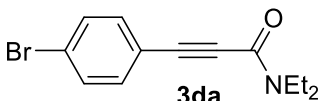
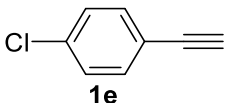
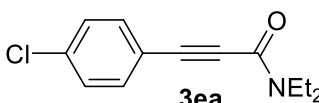
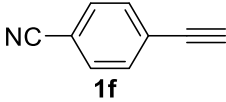
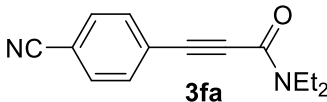
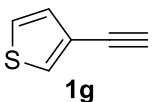
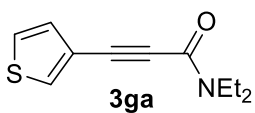
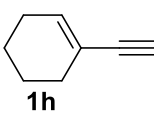
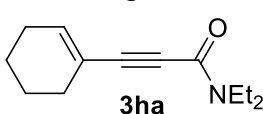
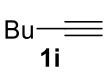
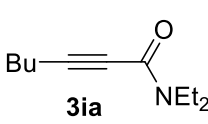
Figure 7. Pd 3d spectra of pristine PdI₄@MWCNT-imi-I and of the catalyst after the parent experiment and catalyst recycles under CO/air = 16/4 atm (left) and 32/8 atm (right) (the other carbonylation conditions are those reported in Table 2).

Thus, as hoped, **PdI₄@MWCNT-imi-I** proved to be a superior catalyst with respect to **PdI₄@MWCNT-imi-Br**, particularly when the process was performed under 32/8 atm of CO/air. This was further confirmed by the results obtained with several other different amines **2b-i** (including piperidine **2f**, substituted piperazines **2g** and **2h**, and *N*-ethylcyclohexanamine **2i**) and 1-alkynes **1a-i** (including phenylacetylenes **1a-f**, 3-ethynylthiophene **1g**, 1-ethynylcyclohex-1-ene **1h**, and 1-hexyne **1i**), as shown in Table 3. We also analyzed some representative products by ICP-MS in order to assess the possible residual content of palladium. The results showed that the percentage of palladium in the final products was lower than 1% in all cases (0.80 % for **3ea**, 0.38% for **3fa**, and 0.21% for **3af**), thus confirming that palladium leaching occurred to a very limited extent under our heterogeneous conditions.

Table 3. PdI₄@MWCNT-imi-I – catalyzed oxidative aminocarbonylation of 1-alkynes **1** with amines **2** to give 2-ynamides **3**.^a



Entry	1	2	3	Yield (%) ^b of 3
1	Ph-C≡C 1a	Et ₂ NH 2a	Ph-C≡C-C(=O)NEt ₂ 3aa	78
2	1a	Bu ₂ NH 2b	Ph-C≡C-C(=O)NBu ₂ 3ab	65
3	1a	 2c	Ph-C≡C-C(=O)N-piperidine 3ac	60
4	1a	 2d	Ph-C≡C-C(=O)N-morpholine 3ad	82
5	1a	 2f	Ph-C≡C-C(=O)N-piperidine 3af	63
6	1a	Me-N-piperazine 2g	Ph-C≡C-C(=O)N-piperazine-Me 3ag	84
7	1a	EtO ₂ C-N-piperazine 2h	Ph-C≡C-C(=O)N-piperazine-CO ₂ Et 3ah	79

8	1a			64
9		2a		77
10		2a		81 (74, 72)
11		2a		80 (74, 68)
12		2a		72
13		2a		78
14		2a		79 (75, 68)
15		2a		74
16		2a		58

^a All reactions were carried out in dioxane (0.25 mmol of **1** per mL of solvent) at 80 °C for 24 h, under 40 atm of a 4:1 mixture of CO-air, in the presence of 2 mol% of Pd and 1.2 equiv of R'₂NH **2**. ^b Isolated yield based on starting **1** (in parentheses, the isolated yields after the first two recycles).

Finally, in order to further confirm that the process took place heterogeneously, we performed a cold filtration test experiment, after stopping the carbonylation of **1c** and **2a** at incomplete **1c** conversion. Thus, in two parallel tests, suspensions of the catalyst **PdI₄@MWCNT-imi-I** in dioxane containing the substrate **1c** and diethylamine **2a** were heated at 80 °C for 6 h with CO (32 atm) and air (8 atm). Then, after cooling to room temperature, one of the two mixtures was filtered through a *Millipore* filter (PTFE, 0.2 μm), the autoclave was loaded with the filtered liquid phase as well as with the CO/air mixture, and the mixture was allowed to react for additional 18 h. At the end of the process, the isolated of **3ca** was 39%. This yield was practically the same of that obtained from the second reaction mixture, from which the product was directly isolated after 6 h (37% yield). This result clearly confirmed that the **PdI₄@MWCNT-imi-I**-catalyzed carbonylation process took place in a heterogeneous fashion.

Conclusions

In conclusions, we have successfully heterogenized our “classical” carbonylation catalyst PdI_2/KI to obtain novel PdI_4^{2-} -based materials **$\text{PdI}_4@\text{MWCNT-imi-X}$** ($X = \text{Br}, \text{I}$). These new heterogeneous catalytic systems have been developed by supporting the catalytically active PdI_4^{2-} anion on an imidazolium network grown on multi-walled carbon nanotubes, and have been fully characterized by advanced techniques (including XPS and TEM).

$\text{PdI}_4@\text{MWCNT-imi-X}$ have proven to be an efficient heterogeneous catalysts in a paradigmatic and particularly important oxidative carbonylation process, that is, the oxidative aminocarbonylation of terminal alkynes to give 2-ynamides (with the material with $X = \text{I}$ being more efficient with respect to that with $X = \text{Br}$). Hot and cold filtration test experiments have confirmed that catalysis occurred in heterogeneous manner, with very limited metal leaching occurring during the reaction as well as at the end of the process, (as confirmed by ICP-MS analysis of representative carbonylation products). Moreover, the catalyst could be easily recycled and, under optimized conditions, showed a good efficiency even after the fourth recycle, when deactivation began to take place owing to the formation of inactive $\text{Pd}(0)$ species, as confirmed by XPS analysis.

Our findings thus open a new way to the efficient immobilization of $\text{Pd}(\text{II})$ catalysts on solid supports, with potential applications not only in carbonylation chemistry, but also in the field of other $\text{Pd}(\text{II})$ -catalyzed processes under heterogeneous conditions.

Experimental Section

General Methods

Solvent and chemicals were reagent grade and were used without further purification. All reactions were analyzed by TLC on silica gel 60 F254 and by GLC using capillary columns with polymethylsilicone + 5% phenylsilicone as the stationary phase. Column chromatography was performed on silica gel 60 (70-230 mesh). Evaporation refers to the removal of solvent under reduced pressure. Melting points are uncorrected. ^1H NMR and $^{13}\text{C}\{^1\text{H}\}$ NMR spectra were recorded at 25 °C on a 300 or 500 MHz spectrometer in CDCl_3 as the solvent and with Me_4Si as internal standard. Chemical shifts (δ) and coupling constants (J) are given in ppm and in Hz, respectively. IR spectra were taken with an FT-IR spectrometer. Mass spectra were obtained using a GC-MS apparatus at 70 eV ionization voltage (normal resolution) and by electrospray ionization mass spectrometry (ESI-MS) (high resolution) with a UHD accurate-mass Q-TOF spectrometer equipped with a Dual AJS ESI source working in positive mode, and were recorded in the 150–1000 m/z range. The LC-MS experimental conditions were as follows: N_2 was employed as desolvation gas at 300 °C and a flow rate of 9 L/min. The nebulizer was set to 45 psig. The Sheat gas temperature was set at 350 °C and a flow of 12 L/min. A potential of 3.5 kV was used on the capillary for positive ion mode. The fragmentor was set to 175 V.

TGA–DSC measurements have been performed in a TGA-DSC 1 Star System by METTLER TOLEDO. The samples were treated in nitrogen or air from room temperature to 100 °C and left at this temperature for 30 minutes in order to eliminate all physisorbed molecules. The temperature was then raised to 1000 °C at 10 °min⁻¹ in N_2 or air (30 mil min⁻¹) and the weight changes were recorded.

The X-ray photoelectron spectroscopy (XPS) analyses were performed with a VG Microtech ESCA 3000 Multilab, equipped with a dual Mg/Al anode. As excitation source was used the Al $K\alpha$ radiation (1486.6 eV). The sample powders were mounted on a double-sided adhesive tape. The pressure in the analysis chamber was in the range of 10⁻⁸ Torr during data collection. The constant charging of the samples was removed by

referencing all the energies to the C 1s binding energy set at 285.1 eV. Analyses of the peaks were performed with the CasaXPS software.

Electron microscopy images were acquired by a FEI-ThermoFisher Versa 3D microscope, operating at 30 kV. 1 mg of each sample was dispersed in 2 mL of toluene and 15 μ L of each suspension was deposited on a 3 mm copper holey carbon coated grid (TAAB); the solvent was evaporated at room temperature overnight. The grids were mounted on a STEM sample holder and the samples were analyzed with 3 different techniques simultaneously: morphological analysis was performed through secondary electron (SE), compositional homogeneity was evaluated by backscattered electrons (BS), while the structural details of the samples were evaluated by transmitted electron (TE).

Preparation of heterogeneous catalysts MWCNT-imi-X (X = Br, I)

imi-Br²³ and **imi-I**¹⁷ were synthesized according to literature procedures.

Synthesis of MWCNT-imi-Br and MWCNT-imi-I

In a two-neck round-bottom flask, pristine MWCNTs (40 mg) and bis-vinylimidazolium salt (1.67 mmol of **imi-Br** or **imi-I**) were suspended in absolute ethanol (13 mL). The suspension was sonicated, under inert atmosphere, for 15 min. The reaction mixture was degassed by bubbling argon for 15 min. When the bis-vinylimidazolium salt was completely solubilized, freshly recrystallized AIBN (0.16 mmol) was added to the reaction mixture, which was in turn stirred and refluxed at 78 °C under argon for 20 h. After this time, the reaction mixture was cooled down to room temperature. **MWCNT-imi-Br** and **MWCNT-imi-I** were recovered by centrifugation and washed with hot MeOH. Before each centrifugation, the solids were sonicated for 15 min in the washing solvent. The last washing was carried out with diethyl ether. The obtained materials **MWCNT-imi-Br** and **MWCNT-imi-I** were dried under vacuum at 60 °C overnight. **MWCNT-imi-Br** (550 mg) was obtained as black solid, whereas **MWCNT-imi-I** (843 mg) as gray solid. Prior to their further use, both the samples **MWCNT-imi-Br** and **MWCNT-imi-I** were intimately crushed in an agate mortar.

Synthesis of Pd₄@MWCNT-Imi-Br

In a two-neck round-bottom flask, a suspension of **MWCNT-Imi-Br** (1 g) in MeCN (67 mL) was sonicated for 10 min. Afterwards, K₂Pd₄ (455.5 mg, 0.658 mmol) was added to the suspension. The reaction mixture was stirred at 60 °C in dark for 20 h. After this time, the solid was recovered by centrifugation and washed several times with hot MeCN, hot MeOH, H₂O, MeOH, MeCN and Et₂O. Before each centrifugation, the suspension of the solid was shortly sonicated. Then, **Pd₄@MWCNT-imi-Br** was dried at 60 °C under vacuum. The final material (1.150 g) was crushed in an agate mortar and obtained as black solid.

Synthesis of Pd₄@MWCNT-imi-I

In a two-neck round-bottom flask, a suspension of **MWCNT-imi-I** (1.5 g) in MeCN (86 mL) was sonicated for 10 min. Afterwards, K₂Pd₄ (585.4 mg, 0.846 mmol) was added to the suspension. The reaction mixture was stirred at 60 °C in dark for 4 days. After this time, the solid was recovered by centrifugation and washed several times with hot MeCN, hot MeOH, H₂O, MeOH, MeCN and Et₂O. Before each centrifugation, the suspension of the solid was shortly sonicated. Then, **Pd₄@MWCNT-imi-I** was dried at 60 °C under vacuum. The final material (1.680 g) was crushed in an agate mortar and obtained as gray solid.

General procedure for the Pd₄@MWCNT-imi-Br – catalyzed oxidative aminocarbonylation of phenylacetylenes 1a-d (Table 2)

A 50 mL stainless-steel autoclave was charged in the presence of air with **Pd₄@MWCNT-imi-Br** (51.2 mg, 4.2 wt% Pd, 2.02×10^{-2} mmol Pd) and a solution of the terminal alkyne **1** (1.0 mmol; **1a**, 102.7 mg; **1b**, 115.8 mg; **1c**, 132.0 mg; **1d**, 181.5 mg) and the secondary amine **2** (1.2 mmol; diethylamine **2a**, 87.8 mg; dibutylamine **2b**, 154.7 mg; pyrrolidine **2c**, 85.6 mg; morpholine **2d**, 104.2 mg) in dioxane (4 mL). The autoclave was sealed and, while the mixture was stirred, was pressurized with CO (16 atm) and air (up to 20 atm). After being stirred at 80°C for 24 h, the autoclave was cooled, degassed and opened. The reaction mixture was taken up with EtOAc until a total volume of ca. 15 mL, and the catalyst was separated from the reaction mixture by centrifugation at 8000 RPM for 15 min. The catalyst was taken up with EtOAc (15 mL), sonicated, separated and washed again with EtOAc (15 mL). After sonication and separation, the catalyst was dried under a high vacuum for 3 h before being resubmitted to the reaction conditions for the recycling experiments. All the supernatant solutions were collected, the solvent was evaporated and the products **3** were purified by column chromatography on silica gel using as eluent hexane–AcOEt from 8:2 to 6:4.

N,N-Diethyl-3-phenylpropiolamide (**3aa**). Yield: 147.5 mg, starting from 102.3 mg of ethynylbenzene (73%, Table 2 entry 1). Yellow oil. IR (film): $\nu = 2214$ (m), 1628 (s), 1427 (m), 1381 (w), 1289 (m), 1219 (w), 1134 (m), 756 (m) cm^{-1} ; ^1H NMR (500 MHz, CDCl_3) δ (ppm): 7.57-7.47 (m, 2H, aromatic), 7.45-7.20 (m, 3H, aromatic), 3.72-3.58 (m, 2H, CH_2CH_3), 3.53-3.40 (m, 2H, CH_2CH_3), 1.32-1.23 (m, 3H, CH_2CH_3), 1.22-1.12 (m, 3H, CH_2CH_3); ^{13}C NMR (125 MHz, CDCl_3) δ (ppm): 154.0, 132.3, 129.9, 128.5, 120.7, 89.0, 81.9, 43.6, 39.3, 14.4, 12.9; GC-MS: $m/z = 201$ (M^+ , 12), 200 (28), 186 (9), 129 (100), 101 (11), 75 (13). The spectroscopic data agreed with those reported.^{12f}

N,N-Dibutyl-3-phenylpropiolamide (**3ab**). Yield: 129.4 mg, starting from 103.0 mg of ethynylbenzene (50%, Table 2 entry 2). Yellow oil. IR (film): $\nu = 2214$ (m), 1628 (s), 1427 (m), 1373 (w), 1304 (m), 1204 (w), 1142 (w), 756 (m) cm^{-1} ; ^1H NMR (500 MHz, CDCl_3) δ (ppm): 7.56-7.51 (m, 2H, aromatic), 7.43-7.33 (m, 3H, aromatic), 3.60 (t, $J = 7.5$, 2H, NCH_2), 3.41 (t, $J = 7.6$, 2H, NCH_2), 1.68-1.60 (m, 2H, $\text{CH}_2\text{CH}_2\text{CH}_3$), 1.60-1.53 (m, 2H, $\text{CH}_2\text{CH}_2\text{CH}_3$), 1.45-1.30 (m, 4H, 2 CH_2CH_3), 0.97 (t, $J = 7.6$, 3H, CH_2CH_3), 0.94 (t, $J = 7.6$, 3H, CH_2CH_3); ^{13}C NMR (125 MHz, CDCl_3) δ (ppm): 154.4, 132.3, 130.0, 128.5, 120.9, 89.2, 82.2, 48.9, 44.6, 31.1, 29.6, 20.2, 20.0, 13.87, 13.86; GC-MS: $m/z = 257$ (M^+ , 5), 215 (19), 214 (39), 130 (18), 129 (100), 75 (7). The spectroscopic data agreed with those reported.⁵

3-Phenyl-1-(pyrrolidin-1-yl)prop-2-yn-1-one (**3ac**). Yield: 126.3 mg, starting from 102.5 mg of ethynylbenzene (63%, Table 2 entry 3). Yellow solid, mp = 52-54°C. IR (KBr): $\nu = 2215$ (m), 1628 (s), 1481 (m), 1420 (m), 1189 (w), 1042 (w), 764 (m) cm^{-1} . ^1H NMR (500 MHz, CDCl_3) δ 7.56-7.52 (m, 2H), 7.43-7.38 (m, 1H), 7.38-7.33 (m, 2H), 3.73 (t, $J = 6.4$, 2 H), 3.53 (t, $J = 6.6$, 2 H), 2.01-1.90 (m, 4 H). ^{13}C NMR (125 MHz, CDCl_3): δ 152.7, 132.4, 130.0, 128.5, 120.7, 88.7, 82.7, 48.2, 45.4, 25.4, 24.7. GC-MS: $m/z = 199$ (M^+ , 33), 170 (18), 143 (12), 129 (100), 116 (15), 102 (21), 75 (19). The spectroscopic data agreed with those reported.^{12f}

1-Morpholino-3-phenylprop-2-yn-1-one (**3ad**). Yield: 122.8 mg, starting from 102.6 mg of ethynylbenzene (57%, Table 2 entry 4). Yellow solid, mp = 55-57 °C. IR (KBr): $\nu = 2214$ (m), 1628 (s), 1489 (w), 1435 (s), 1281 (m), 1211 (m), 1111 (m), 1042 (w), 764 (m) cm^{-1} ; ^1H NMR (500 MHz, CDCl_3) δ (ppm): 7.57-7.53 (m, 2H, aromatic), 7.45-7.40 (m, 1H, aromatic), 7.40-7.35 (m, 2H, aromatic), 3.86-3.82 (m, 2H, morpholine ring), 3.77-3.73 (m, 2H, morpholine ring), 3.70 (s, br, 4H, morpholine ring); ^{13}C NMR (125 MHz, CDCl_3) δ (ppm): 153.3, 132.4, 130.3, 128.7, 120.4, 91.2, 80.9, 67.0, 66.6, 47.4, 42.1; GC-MS: $m/z = 215$ (M^+ , 20), 186 (9), 156 (7), 129 (100), 116 (10), 101 (14), 86 (25). The spectroscopic data agreed with those reported.⁵

N,N-Diethyl-3-(*p*-tolyl)propiolamide (**3ba**). Yield: 143.1 mg, starting from 117.6 mg of 1-ethynyl-4-methylbenzene (66%, Table 2 entry 6). Yellow oil. IR (film): $\nu = 2207$ (m), 1628 (s), 1512 (w), 1427 (m), 1381 (w), 1289 (m), 1219 (w), 1134 (m), 818 (m) cm^{-1} ; ^1H NMR (500 MHz, CDCl_3) δ (ppm): 7.45-7.41 (m, 2H, aromatic), 7.18-7.14 (m, 2H, aromatic), 3.66 (q, $J = 7.2$, 2H, CH_2CH_3), 3.47 (q, $J = 7.2$, 2H, CH_2CH_3), 2.37 (s, 3H, Me), 1.27 (t, $J = 7.2$, 3H, CH_2CH_3), 1.17 (t, $J = 7.2$, 3H, CH_2CH_3); ^{13}C NMR (125MHz, CDCl_3) δ (ppm): 154.2,

140.4, 132.3, 129.3, 117.7, 89.4, 81.6, 43.6, 39.3, 21.6, 14.4, 12.9; GC-MS: m/z = 215 (M^+ , 21), 214 (34), 200 (18), 143 (100), 115 (21), 89 (11). The spectroscopic data agreed with those reported.^{12b}

N,N-Diethyl-3-(4-methoxyphenyl)propiolamide (**3ca**). Yield: 156.4 mg, starting from 131.9 mg of 1-ethynyl-4-methoxybenzene (68%, Table 2 entry 7). Yellow solid, mp = 57-58 °C. IR (KBr): ν = 2207 (m), 1620 (s), 1512 (w), 1381 (m), 1289 (w), 1250 (m), 1173 (w), 1134 (m), 1026 (m), 833 (m) cm^{-1} ; ^1H NMR (500 MHz, CDCl_3) δ (ppm): 7.51-7.46 (m, 2H, aromatic), 6.91-6.85 (m, 2H, aromatic), 3.82 (s, 3H, OMe), 3.66 (q, J = 7.2, 2 H, CH_2CH_3), 3.47 (q, J = 7.2, 2 H, CH_2CH_3), 1.28 (t, J = 7.2, 3H, CH_2CH_3), 1.17 (t, J = 7.2, 3H, CH_2CH_3); ^{13}C NMR (125MHz, CDCl_3) δ (ppm): 160.9, 154.3, 134.1, 114.2, 112.7, 89.5, 81.2, 55.4, 43.6, 39.3, 14.4, 13.0; GC-MS: m/z = 231 (M^+ , 28), 230 (26), 216 (37), 188 (6), 159 (100), 144 (17), 132 (36), 116 (16). The spectroscopic data agreed with those reported.⁵

3-(4-Bromophenyl)-*N,N*-diethylpropiolamide (**3da**). Yield: 176.5 mg, starting from 181.6 mg of 1-bromo-4-ethynylbenzene (63%, Table 2 entry 8). Yellow solid, mp = 92-94 °C. IR (KBr): ν = 2214 (m), 1620 (s), 1481 (m), 1435 (m), 1389 (w), 1296 (m), 1219 (w), 1142 (w), 1072 (m), 1011 (w), 833 (m) cm^{-1} ; ^1H NMR (500 MHz, CDCl_3) δ (ppm): 7.53-7.47 (m, 2H, aromatic), 7.43-7.37 (m, 2H, aromatic), 3.65 (q, J = 7.2, 2H, CH_2CH_3), 3.48 (q, J = 7.2, 2 H, CH_2CH_3), 1.27 (t, J = 7.2, 3H, CH_2CH_3), 1.18 (t, J = 7.2, 3H, CH_2CH_3); ^{13}C NMR (125MHz, CDCl_3) δ (ppm): 153.7, 133.7, 131.9, 124.5, 119.7, 87.8, 82.9, 43.6, 39.4, 14.5, 12.9; GC-MS: m/z = 281 [($M+2$)⁺, 21], 280 [($M+1$)⁺, 45], 279 (M^+ , 21), 278 (44), 266 (19), 264 (20), 209 (96), 207 (100), 128 (47), 100 (28). The spectroscopic data agreed with those reported.⁵

General procedure for the $\text{PdI}_4@\text{MWCNT-imi-I}$ – catalyzed oxidative aminocarbonylation of phenylacetylenes **1a-d** (Table 2)

A 50 mL stainless-steel autoclave was charged in the presence of air with $\text{PdI}_4@\text{MWCNT-imi-I}$ (76.8 mg, 2.8 wt% Pd, 2.02×10^{-2} mmol Pd) and a solution of the terminal alkyne **1** (1.0 mmol; **1a**, 102.7 mg; **1b**, 117.5 mg; **1c**, 132.3 mg; **1d**, 181.7 mg; **1e**, 136.2 mg; **1f**, 127.4 mg; **1g**, 108.4 mg; **1h**, 106.4 mg; **1i**, 81.9 mg) and the secondary amine **2** (1.2 mmol; diethylamine **2a**, 87.6 mg; dibutylamine **2b**, 156.1 mg; pyrrolidine **2c**, 86.2 mg; morpholine **2d**, 104.8 mg; piperidine **2f**, 101.9 mg; *N*-methylpiperazine **2g**, 120.4 mg; ethyl piperazine-1-carboxylate **2h**, 189.4 mg *N*-ethylcyclohexylamine **2i**, 152.7 mg) in dioxane (4 mL). The autoclave was sealed and, while the mixture was stirred, was pressurized with CO (32 atm) and air (up to 40 atm). After being stirred at 80°C for 24 h, the autoclave was cooled, degassed and opened. The reaction mixture was taken up with EtOAc until a total volume of ca. 15 mL, and the catalyst was separated from the reaction mixture by centrifugation at 8000 RPM for 15 min. The catalyst was taken up with EtOAc (15 mL), sonicated, separated and washed again with EtOAc (15 mL). After sonication and separation, the catalyst was dried under a high vacuum for 3 h before being resubmitted to the reaction conditions for the recycling experiments. All the supernatant solutions were collected, the solvent was evaporated and the products **3** were purified by column chromatography on silica gel using as eluent: hexane–AcOEt from 8:2 to 6:4 for **3aa**, **3ab**, **3ac**, **3ad**, **3af**, **3ai**, **3ba**, **3ca**, **3da**, **3ea**, **3fa**, **3ga**, **3ha**; 99:1 CH_2Cl_2 :MeOH for **3ag**; hexane–AcOEt from 7:3 to 1:1 for **3ah**; hexane–AcOEt from 9:1 to 7:3 for **3ia**.

N,N-Diethyl-3-phenylpropiolamide (**3aa**). Yield: 156.4 mg, starting from 102.2 mg of ethynylbenzene (78%, Table 3 entry 1).

N,N-Dibutyl-3-phenylpropiolamide (**3ab**). Yield: 167.9 mg, starting from 102.8 mg of ethynylbenzene (65%, Table 3 entry 2).

3-Phenyl-1-(pyrrolidin-1-yl)prop-2-yn-1-one (**3ac**). Yield: 119.8 mg, starting from 102.7 mg of ethynylbenzene (60%, Table 3 entry 3).

1-Morpholino-3-phenylprop-2-yn-1-one (3ad). Yield: 176.9 mg, starting from 102.0 mg of ethynylbenzene (82%, Table 3 entry 4).

3-Phenyl-1-(piperidin-1-yl)prop-2-yn-1-one (3af). Yield: 133.5 mg, starting from 102.1 mg of ethynylbenzene (63%, Table 3 entry 5). White solid, mp = 101-102°C. IR (KBr): ν = 2214 (w), 1620 (s), 1443 (m), 1281 (m), 1211 (w), 1134 (w), 1026 (m), 764 (m) cm^{-1} . ^1H NMR (500 MHz, CDCl_3) δ (ppm): 7.59-7.50 (m, 2H, aromatic), 7.43-7.31 (m, 3H, aromatic), 3.82-3.73 (m, 2H, piperidine ring), 3.67-3.59 (m, 2H, piperidine), 1.74-1.53 (m, 6H, piperidine); ^{13}C NMR (125 MHz, CDCl_3) δ (ppm): 153.0, 132.3, 129.8, 128.5, 120.9, 90.2, 81.7, 48.2, 42.4, 26.5, 25.4, 24.5; GC-MS: m/z = 213 (M^+ , 33), 212 (33), 184 (17), 156 (7), (100), 101 (13). The spectroscopic data agreed with those reported.²⁴

1-(4-Methylpiperazin-1-yl)-3-phenylprop-2-yn-1-one (3ag). Yield: 191.2 mg, starting from 102.3 mg of ethynylbenzene (84%, Table 3 entry 6). Pale yellow solid, mp = 37-38 °C. IR (KBr): ν = 2214 (m), 1628 (s), 1435 (m), 1296 (m), 1211 (w), 1142 (w), 1042 (w), 1003 (w), 764 (m) cm^{-1} ; ^1H NMR (500 MHz, CDCl_3) δ (ppm): 7.57-7.49 (m, 2H, aromatic), 7.45-7.31 (m, 3H, aromatic), 3.88-3.79 (m, 2H, piperazine ring), 3.74-3.66 (m, 2H, piperazine ring), 2.49-2.44 (m, 2H, piperazine ring), 2.44-2.39 (m, 2H, piperazine ring), 2.33 (s, 3H, CH_3); ^{13}C NMR (125 MHz, CDCl_3) δ (ppm): 153.0, 132.3, 130.0, 128.5, 120.5, 90.6, 81.1, 55.1, 54.4, 47.0, 46.0, 41.4; GC-MS: m/z = 228 (M^+ , 9), 227 (11), 199 (11), 185 (21), 156 (7), 129 (48), 99 (51), 83 (47), 70 (100). The spectroscopic data agreed with those reported.^{12a}

Ethyl 4-(3-phenylpropioloyl)piperazine-1-carboxylate (3ah). Yield: 227.4 mg, starting from 102.5 mg of ethynylbenzene (79%, Table 3 entry 7). Grayish solid, mp = 73-74 °C. IR (KBr): ν = 2214 (m), 1697 (s), 1628 (s), 1427 (s), 1289 (w), 1234 (m), 1204 (w), 1080 (w), 1034 (w), 988 (w), 764 (m) cm^{-1} ; ^1H NMR (500 MHz, CDCl_3) δ (ppm): 7.57-7.52 (m, 2H, aromatic), 7.45-7.40 (m, 1H, aromatic), 7.40-7.34 (m, 2H, aromatic), 4.26-4.10 (m, 2H, $\text{CO}_2\text{CH}_2\text{CH}_3$), 3.86-3.78 (m, 2H, piperazine ring), 3.72-3.65 (m, 2H, piperazine ring), 3.61-3.52 (m, 2H, piperazine ring), 3.53-3.47 (m, 2H, piperazine ring), 1.28 (t, J = 7.1, 3H, $\text{CO}_2\text{CH}_2\text{CH}_3$); ^{13}C NMR (125 MHz, CDCl_3) δ (ppm): 155.4, 153.2, 132.4, 130.2, 128.6, 120.4, 91.2, 81.0, 61.8, 46.8, 44.1, 43.4, 41.4, 14.6; GC-MS: m/z = 286 (M^+ , 6), 257 (6), 197 (39), 157 (26), 129 (100), 116 (42), 85 (15). HRMS-ESI (m/z): $[(\text{M}+\text{H})^+]$ calcd for $(\text{C}_{16}\text{H}_{19}\text{N}_2\text{O}_3)^+$: 287.1390; found, 287.1383.

N-Cyclohexyl-N-ethyl-3-phenylpropiolamide (3ai). Yield: 164.4 mg, starting from 102.7 mg of ethynylbenzene (64%, Table 3 entry 8). Yellow oil. IR (film): ν = 2932 (s), 2855 (m), 2214 (m), 1620 (s), 1420 (m), 1312 (m), 1227 (w), 1150 (w), 1111 (m), 1026 (w), 895 (w), 756 (m), 694 (m) cm^{-1} ; ^1H NMR (500 MHz, CDCl_3) (mixture of stereoisomers A and B deriving from slow rotation around the amide bond; A/B ratio ca. 1.4) δ (ppm): 7.56-7.51 [m, aromatic, 2H (A) + 2H (B)], 7.44-7.33 [m, aromatic, 3H (A) + 3H (B)], 4.34 [tt, J = 11.7, 3.4, NCH, 1H (B)], 4.26 [tt, J = 11.9, 3.5, NCH, 1H (A)], 3.58 [q, J = 7.1, NCH₂, 2H (B)], 3.39 [q, J = 7.1, NCH₂, 2H (A)], 1.93-1.63 [m, cyclohexyl ring, 6H (A) + 6H (B)], 1.57-1.30 [m, cyclohexyl ring, 4H (A) + 4H (B)], 1.33 [t, J = 7.1, 3H, NCH₂CH₃, (B)], 1.19 [t, J = 7.1, 3 H, NCH₂CH₃, (A)]; ^{13}C NMR (125 MHz, CDCl_3) δ (ppm): 154.5, 154.2, 132.4, 130.0, 128.5, 121.0, 89.3, 88.7, 82.8, 82.2, 39.9, 36.5, 31.9, 30.8, 26.1, 25.8, 25.6, 25.3, 16.8, 14.7; GC-MS: m/z = 255 (M^+ , 10), 254 (10), 212 (14), 174 (20), 129 (100), 101 (9). HRMS-ESI (m/z): $[(\text{M}+\text{H})^+]$ calcd for $(\text{C}_{17}\text{H}_{22}\text{NO})^+$: 256.1696; found, 256.1684.

N,N-Diethyl-3-(p-tolyl)propiolamide (3ba). Yield: 166.6 mg, starting from 117.5 mg of 1-ethynyl-4-methylbenzene (77%, Table 3 entry 9).

N,N-Diethyl-3-(4-methoxyphenyl)propiolamide (3ca). Yield: 186.9 mg, starting from 132.3 mg of 1-ethynyl-4-methoxybenzene (81%, Table 3 entry 10).

3-(4-Bromophenyl)-N,N-diethylpropiolamide (3da). Yield: 224.3 mg, starting from 181.7 mg of 1-bromo-4-ethynylbenzene (80%, Table 3 entry 11).

3-(4-Chlorophenyl)-N,N-diethylpropiolamide (3ea). Yield: 168.7 mg, starting from 136.2 mg of 1-chloro-4-ethynylbenzene (72%, Table 3 entry 12). Yellow solid, mp = 62-63 °C. IR (KBr): ν = 2222 (m), 1628 (s), 1489 (m), 1427 (m), 1381 (w), 1289 (m), 1219 (w), 1134 (w), 1088 (m), 1011 (w), 833 (m) cm^{-1} . ^1H NMR (500 MHz, CDCl_3) δ (ppm): 7.50-7.42 (m, 2H, aromatic), 7.39-7.30 (m, 2H, aromatic), 3.-71-3.59 (m, 2H, CH_2CH_3), 3.53-3.42 (m, 2 H, CH_2CH_3), 1.27 (t, J = 6.9, 3H, CH_2CH_3), 1.18 (t, J = 6.8, 3H, CH_2CH_3); ^{13}C NMR (125 MHz, CDCl_3) δ (ppm): 153.7, 136.2, 133.5, 129.0, 119.4, 87.7, 83.0, 43.6, 39.4, 14.4, 12.8; GC-MS: m/z = 237 [(M+2)⁺, 5], 236 [(M+1)⁺, 14], 235 (M⁺, 18), 234 (37), 220 (15), 165 (37), 163 (100), 136 (8), 99 (22). The spectroscopic data agreed with those reported.^{12f}

3-(4-Cyanophenyl)-N,N-diethylpropiolamide (3fa). Yield: 177.1 mg, starting from 127.4 mg of 4-ethynylbenzotrile (78%, Table 3 entry 13). Yellow solid, mp = 92-93 °C. IR (KBr): ν = 2222 (m), 1620 (s), 1435 (m), 1281 (w), 1219 (w), 1103 (w), 1018 (w), 833 (m) cm^{-1} ; ^1H NMR (500 MHz, CDCl_3) δ (ppm): 7.70-7.58 (m, 4H, aromatic), 3.69-3.60 (m, 2H, CH_2CH_3), 3.53-3.44 (m, 2 H, CH_2CH_3), 1.29 (t, J = 6.8, 3H, CH_2CH_3), 1.19 (t, J = 6.8, 3H, CH_2CH_3); ^{13}C NMR (125 MHz, CDCl_3) δ (ppm): 153.2, 132.8, 132.2, 125.7, 118.0, 113.4, 86.6, 85.5, 43.7, 39.6, 14.5, 12.8; GC-MS: m/z = 226 (M⁺, 13), 225 (29), 211 (11), 154 (100). The spectroscopic data agreed with those reported.⁵

N,N-Diethyl-3-(thiophen-3-yl)propiolamide (3ga). Yield: 163.4 mg, starting from 108.4 mg of 3-ethynylthiophene (79%, Table 3 entry 14). Yellow oil. IR (film): ν = 2214 (m), 1620 (s), 1427 (m), 1281 (m), 1134 (w), 787 (m) cm^{-1} . ^1H NMR (500 MHz, CDCl_3) δ (ppm): 7.65 (dd, J = 2.9, 0.7, 1H, H-2 on thiophene ring), 7.31 (dd, J = 5.0, 2.9, 1H, H-4 on thiophene ring), 7.19 (dd, J = 5.0, 0.7, 1H, H-5 on thiophene ring), 3.65 (q, J = 7.2, 2H, CH_2CH_3), 3.47 (q, J = 7.2, 2 H, CH_2CH_3), 1.27 (t, J = 7.2, 3H, CH_2CH_3), 1.17 (t, J = 7.2, 3H, CH_2CH_3); ^{13}C NMR (125 MHz, CDCl_3) δ (ppm): 154.0, 131.8, 129.9, 125.9, 119.9, 84.5, 81.8, 43.6, 39.3, 14.4, 12.9; GC-MS: m/z = 207 (M⁺, 14), 192 (11), 135 (100), 108 (8). The spectroscopic data agreed with those reported.^{12f}

3-(Cyclohex-1-en-1-yl)-N,N-diethylpropiolamide (3ha). Yield: 151.3 mg, starting from 106.4 mg of 1-ethynylcyclohex-1-ene (74%, Table 3 entry 15). Yellow oil. IR (film): ν = 2199 (m), 1628 (s), 1458 (m), 1427 (m), 1373 (w), 1281 (m), 1219 (w), 1126 (m), 795 (w) cm^{-1} . ^1H NMR (500 MHz, CDCl_3) δ (ppm): 6.36-6.31 (m, 1H, =CH), 3.57 (q, J = 7.1, 2H, CH_2CH_3), 3.43 (q, J = 7.1, 2H, CH_2CH_3), 2.22-2.10 (m, 4H, cyclohexyl ring), 1.70-1.56 (m, 4H, cyclohexyl ring), 1.22 (t, J = 7.1, 3H, CH_2CH_3), 1.14 (t, J = 7.1, 3H, CH_2CH_3); ^{13}C NMR (125 MHz, CDCl_3) δ (ppm): 154.4, 139.5, 119.2, 91.1, 79.8, 43.5, 39.2, 28.4, 25.8, 22.0, 21.2, 14.3, 12.9; GC-MS: m/z = 205 (M⁺, 27), 204 (27), 190 (23), 176 (8), 162 (8), 133 (100), 105 (29), 91 (17), 79 (32). HRMS-ESI (m/z): [(M+H)⁺] calcd for ($\text{C}_{13}\text{H}_{20}\text{NO}$)⁺: 206.1539; found, 206.1523.

N,N-Diethylhept-2-ynamide (2ia). Yield: 89.5 mg, starting from 81.9 mg of hex-1-yne (50%, Table 3 entry 16). Yellow oil. IR (film): ν = 2222 (m), 1628 (s), 1458 (m), 1427 (m), 1381 (w), 1319 (w), 1281 (m), 1219 (w), 1173 (w), 1080 (m), 741 (m) cm^{-1} . ^1H NMR (500 MHz, CDCl_3) δ (ppm): 3.57 (q, J = 7.1, 2H, CH_2CH_3), 3.41 (q, J = 7.2, 2H, CH_2CH_3), 2.36 (t, J = 7.1, 2H $\equiv\text{CCH}_2$), 1.60-1.52 (m, 2H, $\text{CH}_2\text{CH}_2\text{CH}_3$), 1.48-1.38 (m, 2H, CH_2CH_3), 1.21 (t, J = 7.1, 3H, CH_3), 1.13 (t, J = 7.2, 3H, CH_3), 0.93 (t, J = 7.3, 3H, CH_3); ^{13}C NMR (125 MHz, CDCl_3) δ (ppm): 154.2, 91.8, 74.4, 43.5, 39.1, 29.9, 22.0, 18.6, 14.3, 13.5, 12.9; GC-MS: m/z = 181 (M⁺, 5), 166 (13), 152 (14), 138 (48), 124 (24), 109 (100), 79 (42). The spectroscopic data agreed with those reported.^{12b}

Hot filtration test

A mixture of phenylacetylene **1a** (103.3 mg, 1.0 mmol), diethylamine **2a** (1.2 mmol, 86.8 mg), and **Pd₄@MWCNT-imi-Br** (51.2 mg, 4.2 wt% Pd, 2.02×10^{-2} mmol Pd) in dioxane (4 mL) was stirred in a sealed tube at 80°C for 1 h. The reaction mixture was filtered while hot using a pre-heated *Millipore* filter (0.2 μm in PTFE), and a 50 mL autoclave was charged with the filtrate. The autoclave was sealed and, while the mixture was stirred, was pressurized with CO (16 atm) and air (up to 20 atm). After being stirred at 80°C for 24 h, the autoclave was cooled, degassed and opened. The reaction crude was analyzed by GLC-MS, which

evidenced the formation of *N,N*-diethyl-3-phenylpropiolamide **3aa** in only 5% GLC yield (using eicosane as internal standard).

Cold filtration test

Two parallel tests were carried out:

Experiment A: A 50 mL stainless-steel autoclave was charged in the presence of air with **Pdl₄@MWCNT-imi-I** (50.7 mg, 2.8 wt% Pd, 1.3×10^{-2} mmol Pd) and a solution of 1-ethynyl-4-methoxybenzene **1c** (85.8 mg, 0.65 mmol) and diethylamine **2a** (57.5 mg, 0.79 mmol,) in dioxane (2.6 mL). The autoclave was sealed and, while the mixture was stirred, the autoclave was pressurized with CO (32 atm) and air (up to 40 atm). After being stirred at 80°C for 6 h, the autoclave was cooled, degassed and opened. The reaction mixture was taken up with EtOAc until a total volume of ca. 15 mL, and the catalyst was separated from the reaction mixture by centrifugation at 8000 RPM for 15 min. The catalyst was taken up with EtOAc (15 mL), sonicated, separated and washed again with EtOAc (15 mL). All the supernatant solutions were collected, the solvent was evaporated and the product **3ca** was purified by column chromatography on silica gel using as eluent hexane–AcOEt from 8:2 to 6:4 (yield: 56.2 mg, 37%).

Experiment B: A 50 mL stainless-steel autoclave was charged in the presence of air with **Pdl₄@MWCNT-imi-I** (50.0 mg, 2.8 wt% Pd, 1.3×10^{-2} mmol Pd) and a solution of **1c** (86.6 mg, 0.66 mmol) and **2a** (57.1 mg, 0.78 mmol) in dioxane (2.6 mL). The autoclave was sealed and, while the mixture was stirred, the autoclave was pressurized with CO (32 atm) and air (up to 40 atm). After being stirred at 80°C for 6 h, the autoclave was cooled, degassed and opened. The mixture was filtered through a *Millipore* filter (PTFE, 0.2 μm), the autoclave was loaded again with the filtered liquid phase and pressurized with CO (32 atm) and air (up to 40 atm). The mixture was then allowed to react at 80°C for additional 18 h. At the end of the process, the autoclave was cooled, degassed and opened. The solvent was evaporated, and product **3ca** was purified by column chromatography on silica gel using as eluent hexane–AcOEt from 8:2 to 6:4 (yield: 59.1 mg, 39%).

References

- Gabriele, B. (Ed.) *Carbon Monoxide in Organic Synthesis: Carbonylation Chemistry*; Wiley-VCH: Weinheim, Germany, 2021; ISBN 9783527347957.
- For recent reviews, see: (a) Shaifali; Sheetal, Das, P. Supported palladium catalyzed carbonylative coupling reactions using carbon monoxide as C1 source. *Chem. Rec.* **2022**, *22*, e2021001. (b) Shi, Y.; Xia, C.; Huang, Y.; He, L. Electrochemical approaches to carbonylative coupling reactions. *Chem. Asian J.* **2021**, *16*, 2830-3841. (c) Botla, V.; Voronov, A.; Motti, E.; Carfagna, C.; Mancuso, R.; Gabriele, B.; Della Ca', N. Advances in visible-light-mediated carbonylative reactions via carbon monoxide (CO) incorporation. *Catalysts* **2021**, *11*, 918. (d) Cheng, L.-J.; Mankad, N.P. Copper-catalyzed carbonylative coupling of alkyl halides. *Acc. Chem. Res.* **2021**, *54*, 2261-2274. (e) Tan, Y.; Lang, J.; Tang, M.; Li, J.; Mi, P.; Zheng, X. N-Formylsaccharin as a CO source: Applications and recent developments. *ChemistrySelect* **2021**, *6*, 2343-2349. (f) Cai, S.; Zhang, H.; Huang, H. Transition-metal-catalyzed hydroaminocarbonylations of alkenes and alkynes. *Trends Chem.* **2021**, *3*, 218-230. (g) Sang, R.; Hu, Y.; Razaq, R.; Jackstell, R.; Franke, R.; Beller, M. State-of-the-art palladium-catalyzed alkoxy carbonylations. *Org. Chem. Front.* **2021**, *8*, 799-811. (h) Lukasevics, L.; Grigorjeva, L. Cobalt-catalyzed carbonylation of the C-H bond. *Org. Biomol. Chem.* **2020**, *18*, 7460-7466. (i) Das, D.; Bhanage, B.M. Double carbonylation reactions: Overview and recent advances. *Adv. Synth. Catal.* **2020**, *362*, 3022-3058. (j) Peng, J.B. Recent advances in carbonylative difunctionalization of

alkenes. *Adv. Synth. Catal.* **2020**, *362*, 3059-3080. (k) Chen, Z.; Wang, L.-C.; Wu, X.-F. Carbonylative synthesis of heterocycles involving diverse CO surrogates. *Chem. Commun.* **2020**, *56*, 6016-6030. (l) Yin, Z.; Xu, J.; Wu, X.-F. No making without breaking: Nitrogen-centered carbonylation reactions. *ACS Catal.* **2020**, *10*, 6510-6531. (m) Zhang, S.; Neumann, H.; Beller, M. Synthesis of α,β -unsaturated carbonyl compounds by carbonylation reactions. *Chem. Soc. Rev.* **2020**, *49*, 3187-3210. (n) Jones, D.J.; Lautems, M.; McGlacken, G.P. The emergence of Pd-mediated reversible oxidative addition in cross coupling, carbohalogenation and carbonylation reactions. *Nat. Catal.* **2019**, *2*, 843-851. (o) Peng, J.B.; Geng, H.-Q.; Wu, X.-F. The chemistry of CO: Carbonylation. *Chem* **2019**, *5*, 526-552.

3. Gabriele, B.; Costa, M.; Salerno, G.; Chiusoli, G.P. A new synthesis of trimethyl acetonate by palladium-catalysed triple carbonylation of propynyl alcohol. *J. Chem. Soc., Chem. Commun.* **1992**, 1007-1008.

4. Gabriele, B.; Costa, M.; Salerno, G.; Chiusoli, G.P. An efficient and selective palladium-catalysed oxidative dicarbonylation of alkynes to alkyl- or aryl-maleic esters. *J. Chem. Soc., Perkin Trans.* **1994**, 83-87.

5. Gabriele, B.; Salerno, G.; Veltri, L. Costa, M. Synthesis of 2-ynamides by direct palladium-catalyzed oxidative aminocarbonylation of alk-1-ynes. *J. Organomet. Chem.* **2001**, *622*, 84-88.

6. Gabriele B.; Veltri, L.; Salerno, G.; Costa, M.; Chiusoli, G.P. Synthesis of maleic anhydrides and maleic acids by Pd-catalyzed oxidative dicarbonylation of alk-1-ynes. *Eur. J. Org. Chem.* **2003**, 1722-1728.

7. For accounts and reviews, see: (a) Mancuso, R.; Della Ca, N.; Veltri, L.; Ziccarelli, I.; Gabriele, B. PdI₂-based catalysis for carbonylation reactions: A personal account. *Catalysts* **2019**, *9*, 610. (b) Gabriele, B. Recent advances in the PdI₂-catalyzed carbonylative synthesis of heterocycles from acetylenic substrates: A personal account. *Targets Heterocycl Syst.* **2018**, *22*, 41-55. (c) Gabriele, B. Synthesis of heterocycles by palladium-catalyzed carbonylative reactions. In *Advances in Transition-Metal Mediated Heterocyclic Synthesis*; Solé, D., Fernández, I., Eds.; Academic Press-Elsevier: London, UK, 2018; Volume 3, pp. 55-127. (d) Gabriele, B.; Mancuso, R.; Salerno, G. Oxidative carbonylation as a powerful tool for the direct synthesis of carbonylated heterocycles. *Eur. J. Org. Chem.* **2012**, 6825-6839. (e) Gabriele, B.; Salerno, G.; Costa, M. Oxidative Carbonylations. *Top. Organomet. Chem.* **2006**, *18*, 239-272. (f) Gabriele, B.; Salerno, G. PdI₂. In *e-EROS (Electronic Encyclopedia of Reagents for Organic Synthesis)*; Crich, D., Ed.; Wiley-Interscience: New York, NY, USA, 2006. (g) Gabriele, B.; Salerno, G.; Costa, M.; Chiusoli, G.P. Recent advances in the synthesis of carbonyl compounds by palladiumcatalyzed oxidative carbonylation reactions of unsaturated substrates. *Curr. Org. Chem.* **2004**, *8*, 919-946. (h) Gabriele, B.; Salerno, G.; Costa, M.; Chiusoli, G.P. Recent developments in the synthesis of heterocyclic derivatives by PdI₂-catalyzed oxidative carbonylation reactions. *J. Organomet. Chem.* **2003**, *687*, 219-228.

8. For some very recent examples, see: (a) Mancuso, R.; Ziccarelli, I.; Novello, M.; Cuocci, C.; Centore, R.; Della Ca', N.; Olivieri, D.; Carfagna, C.; Gabriele, B. A palladium iodide catalyzed regioselective carbonylative route to isocoumarin and thienopyranone carboxylic esters. *J. Catal.* **2022**, *405*, 164-182. (b) Mancuso, R.; Lettieri, M.; Ziccarelli, I.; Russo, P.; Palumbo Piccionello, A.; Gabriele, B. Multicomponent synthesis of benzothiophen-2-acetic esters by a palladium iodide catalyzed S-cyclization – alkoxy carbonylation sequence. *Adv. Synth. Catal.* **2021**, *363*, 4612-4620. (c) Mancuso, R.; Strangis, R.; Ziccarelli, I.; Della Ca', N.; Gabriele, B. Palladium catalysis with sulfurated substrates under aerobic conditions: A direct carbonylation approach to thiophene-3-carboxylic esters. *J. Catal.* **2021**, *393*, 335-343.

9. Arai, M.; Zhao, F. Metal catalysts recycling and heterogeneous/homogeneous catalysis. *Catalysts* **2015**, *5*, 868-870.

10. (a) Su, D. S.; Perathoner, S.; Centi, G. Nanocarbons for the Development of Advanced Catalysts. *Chem. Rev.* **2013**, *113*, 5782-5816; (b) Melchionna, M.; Marchesan, S.; Prato, M.; Fornasiero, P. Carbon nanotubes and catalysis: the many facets of a successful marriage. *Catal. Sci. Technol.* **2015**, *5*, 3859-3875; (c)

Campisciano, V.; Gruttadauria, M.; Giacalone, F. Modified Nanocarbons for Catalysis. *ChemCatChem* **2019**, *11*, 90-133.

11. (a) Campisciano, V.; Calabrese, C.; Liotta, L.F.; La Parola, V.; Gruttadauria, M.; Giacalone, F. Templating effect of carbon nanoforms on highly cross-linked imidazolium network: Catalytic activity of the resulting hybrids with Pd nanoparticles. *App. Organomet. Chem.* **2019**, *33*, e4848; (b) Campisciano, V.; Burger, R.; Calabrese, C.; Liotta, L.F.; Lo Meo, P.; Gruttadauria, M.; Giacalone, F. Straightforward preparation of highly loaded MWCNT–polyamine hybrids and their application in catalysis. *Nanoscale Adv.* **2020**, *2*, 4199-4211; (c) Campisciano, V., Valentino, L., Morena, A., Santiago-Portillo, A.; Saladino, N.; Gruttadauria, M.; Aprile, C., Giacalone, F. Carbon nanotube supported aluminum porphyrin-imidazolium bromide crosslinked copolymer: A synergistic bifunctional catalyst for CO₂ conversion. *J. CO₂ Util.* **2022**, *57*, 101884.

12. (a) Gadge, S.T.; Khedkar, M.V.; Lanke, S.R.; Bhanage, B.M. Oxidative aminocarbonylation of terminal alkynes for the synthesis of alk-2-ynamides by using palladium-on-carbon as efficient, heterogeneous, phosphine-free, and reusable catalyst. *Adv. Synth. Catal.* **2012**, *354*, 2049-2056; (b) Zhang, C.; Liu, J.; Xia, C. Palladium–N-heterocyclic carbene (NHC) catalyzed synthesis of 2-ynamides via oxidative aminocarbonylation of alkynes with amines. *Catal. Sci. Technol.* **2015**, *5*, 4750-4754. (c) Idris, M.A.; Kim, M.; Kim, J.G.; Lee, S. Palladium-catalyzed decarboxylative aminocarbonylation with alkynoic acid and tertiary amine for the synthesis of alkynyl amide. *Tetrahedron* **2019**, *75*, 4130-4137. (d) Hwang, J.; Choi, J.; Park, K.; Kim, W.; Song, K.H.; Lee, S. Palladium-catalyzed oxidative aminocarbonylation by decarboxylative coupling: Synthesis of alkynyl amides. *Eur. J. Org. Chem.* **2015**, 2235-2243. (e) Zeng, L.; Li, H.; Hu, J.; Zhang, D.; Hu, J.; Peng, P.; Wang, S.; Shi, R.; Peng, J.; Pao, C.-W.; Chen, J.-L.; Lee, J.-F.; Zhang, H.; Chen, Y.-H.; Lei, A. Electrochemical oxidative aminocarbonylation of terminal alkynes. *Nat. Catal.* **2020**, *3*, 438-445. (f) Hughes, N.L.; Brown, C.L.; Irwin, A.A.; Cao, Q.; Muldoon, M.J. Palladium(II)-catalysed aminocarbonylation of terminal alkynes for the synthesis of 2-ynamides: addressing the challenges of solvents and gas mixtures. *ChemSusChem* **2017**, *10*, 675-680.

13. (a) Rudolf, W.-D.; Schwarz, R. A New Approach to 5-Arylidene-thiazolidin-4-ones. *Heterocycles*, **1986**, *24*, 3459-3465; (b) Pinto, A.; Neuville, L.; Retailleau, P.; Zhu, J. P. Synthesis of 3-(Diarylmethylenyl)oxindole by a Palladium-Catalyzed Domino Carbopalladation/C–H Activation/C–C Bond-Forming Process. *Org. Lett.*, **2006**, *8*, 4927–4930; (c) Eichner, S.; Eichner, T.; Floss, H. G.; Fohrer, J.; Hofer, E.; Sasse, F.; Zeilinger, C.; Kirschning, A. Broad Substrate Specificity of the Amide Synthase in *S. hygrosopicus*—New 20-Membered Macrolactones Derived from Geldanamycin. *J. Am. Chem. Soc.*, **2012**, *134*, 1673–1679.

14. (a) Hay, L. A.; Koenig, T. M.; Gina, F. O.; Copp, J. D.; Mitchell, D. Palladium-Catalyzed Hydroarylation of Propiolamides. A Regio- and Stereocontrolled Method for Preparing 3,3-Diarylacrylamides. *J. Org. Chem.* **1998**, *63*, 5050-5058; (b) Brennfuhrer, A.; Neumann, H.; Beller, M. Palladium-Catalyzed Carbonylation Reactions of Aryl Halides and Related Compounds. *Angew. Chem., Int. Ed.*, **2009**, *48*, 4114–4133; (c) Wu, W. T.; Zhang, Z. H.; Liebeskind, L. S. *J. Am. Chem. Soc.* **2011**, *133*, 14256–14259.

15. The flammability range for CO–O₂ mixture is 16.7–93.5% at room temperature and it becomes even larger at higher temperatures. See: Bartish, C.M.; Drissel, G.M. In *Kirk-Othmer Encyclopedia of Chemical Technology*, 3rd ed.; Grayson, M., Eckroth, D., Bushey, G. J., Campbell, L., Klingsberg, A., van Nes, L., Eds.; Wiley-Interscience: New York, 1978; Vol. 4, p 774.

16. For recent examples, see: (a) Veltri, L.; Russo, P.; Prestia, T.; Vitale, P.; Romeo, R.; Gabriele, B. A multicomponent palladium-catalyzed carbonylative approach to imidazopyridinyl-*N,N*-dialkylacetamides. *J. Catal.* **2020**, *386*, 53-59. (b) Veltri, L.; Giofré, S.V.; Devo, P.; Romeo, R.; Dobbs, A.P.; Gabriele, B. A palladium iodide-catalyzed oxidative aminocarbonylation-heterocyclization approach to functionalized benzimidazoimidazoles. *J. Org. Chem.* **2018**, *83*, 1680-1685. (c) Mancuso, R.; Veltri, L.; Russo, P.; Grasso, G.;

- Romeo, R.; Gabriele, B. Palladium-catalyzed carbonylative synthesis of functionalized benzimidazopyrimidinones. *Synthesis* **2018**, *50*, 267-277.
17. Calabrese, C.; Liotta, L. F.; Carbonell, E.; Giacalone, F.; Gruttadauria, M., Aprile, C. Imidazolium-Functionalized Carbon Nanohorns for the Conversion of Carbon Dioxide: Unprecedented Increase of Catalytic Activity after Recycling. *ChemSusChem* **2017**, *10*, 1202-1209.
18. (a) Campisciano, V.; La Parola, V.; Liotta, L. F.; Giacalone, F., Gruttadauria, M. Fullerene-ionic-liquid conjugates: A new class of hybrid materials with unprecedented properties. *Chem. Eur. J.* **2015**, *21*, 3327-3334; (b) Giacalone, F.; Campisciano, V.; Calabrese, C.; La Parola, V.; Syrgiannis, Z.; Prato, M.; Gruttadauria, M. Single-Walled Carbon Nanotube–Polyamidoamine Dendrimer Hybrids for Heterogeneous Catalysis. *ACS Nano* **2016**, *4*, 4627–4636.
19. Eriksson, S.; Boutonnet, M.; Järås, S. Catalytic Combustion of Methane in Steam and Carbon Dioxide-Diluted Reaction Mixtures. *Appl. Catal., A* **2006**, *312*, 95–101.
20. (a) Giacalone, F.; Campisciano, V.; Calabrese, C.; La Parola, V.; Liotta, L. F.; Aprile, C.; Gruttadauria, M. Supported C₆₀-IL-PdNPs as extremely active nanocatalysts for C–C cross-coupling reactions, *J. Mater. Chem. A*, **2016**, *4*, 17193-17206; (b) Xu, M; Zhao, J.; Shu, G.; Zheng, X.; Liu, Q. Wang, Y.; Zeng, M. One-pot carbonization of chitosan/P123/PdCl₂ blend hydrogel membranes to N-doped carbon supported Pd catalytic composites for Ullmann reactions. *Int. J. Biol. Macromol.* **2019**, *125*, 213-220.
21. These conditions were outside the explosion limits for CO–air mixtures. The flammability limits for CO in air are ca. 16–70% at 18–20 °C and atmospheric pressure and tend to decrease at higher total pressure. See: Bartish, C. M.; Drissel, G. M. In *Kirk–Othmer Encyclopedia of Chemical Technology*, 3rd ed.; Grayson, M., Eckroth, D., Bushey, G. J., Campbell, L., Klingsberg, A., van Nes, L., Eds.; Wiley-Interscience: New York, 1978; Vol. 4, p 7750.
22. Gabriele, B.; Costa, M.; Salerno, G.; Chiusoli, G.P. An efficient and selective palladium-catalysed oxidative dicarbonylation of alkynes to alkyl-or aryl-maleic esters. *J. Chem. Soc., Perkin Trans. 1* **1994**, 83-87.
23. (a) Montroni, E.; Lombardo, M.; Quintavalla, A.; Trombini, C.; Gruttadauria, M.; Giacalone, F. A Liquid–Liquid Biphasic Homogeneous Organocatalytic Aldol Protocol Based on the Use of a Silica Gel Bound Multilayered Ionic Liquid Phase. *ChemCatChem* **2012**, *4*, 1000-1006; (b) Pavia, C.; Giacalone, F.; Bivona, L. A.; Salvo, A. M. P.; Petrucci, C.; Strappaveccia, G.; Vaccaro, L.; Aprile, C.; Gruttadauria, M. Evidences of release and catch mechanism in the Heck reaction catalyzed by palladium immobilized on highly cross-linked-supported imidazolium salts. *J. Mol. Catal. A*, **2014**, *387*, 57–62.
24. Fiore, V. A.; Maas, G. *N*-triflyl-propiolamides: Preparation and transamidation reactions. *Tetrahedron* **2019**, *75*, 3586-3595.